Low Energy ECG Features Extraction for Atrial Fibrillation Detection in Wearable Sensors

Manan AlMusallam[1] and Adel Soudani[2]

[1]Department of Computer Science, Imam Mohammad Bin Saud Islamic University, Riyadh, Saudi Arabia
[2]Department of Computer Science, King Saud University, Riyadh, Saudi Arabia

Keywords: ECG Signal Processing, Atrial Fibrillation, Wavelet Analysis, Features Extraction, WBSN.

Abstract: The Internet of Health Things plays a key role in the transformation of health care systems as it enables wearable health monitoring systems to ensure continuous and non-invasive tracking of vital body parameters. To successfully detect the cardiac problem of Atrial Fibrillation (AF) wearable sensors are required to continuously sense and transmit ECG signals. The traditional approach of ECG streaming over energy-consuming wireless links can overwhelm the limited energy resources of wearable sensors. This paper proposes a low-energy features' extraction method that combines the RR interval and P wave features for higher AF detection accuracy. In the proposed scheme, instead of streaming raw ECG signals , local AF features extraction is executed on the sensors. Results have shown that combining time-domain features with wavelet extracted features, achieved a sensitivity of 98.59% and a specificity of 97.61%. In addition, compared to ECG streaming, on-sensor AF detection achieved a 92% gain in energy savings.

1 INTRODUCTION

Atrial fibrillation (AF) is a prevalent arrhythmia that is associated with an increased mortality, increased hospitalization rate, and a higher risk of strokes. Moreover, its prevalence is expected to increase significantly in the next years due to an ageing population (Mairesse et al., 2018). A major challenge in AF diagnosis is that its early stages episodes are short self-terminating with little or no symptoms experienced by the patient. The electrocardiogram (ECG) (Petty, 2016), a graphical representation of the heart's electrical activity, is an essential tool in AF diagnosis. However, standard ECG recordings that are done in hospitals provide only a snapshot of the heart's activity. Therefore, AF can go undiagnosed until a patient has a routine checkup or suffer from a serious complication such as a stroke. Ambulatory ECG monitoring is an alternative tool for AF diagnosis where ECG recordings are acquired, outside of hospitals, over a pro-longed period of time. Thus, it can capture short-lived and silent episodes of AF.

However, traditional ECG recorders cannot provide real time ECG monitoring because patients are required to bring the recorder back to the doctor office for analysis. Recent technology advances resulted in the development of wearable ECG monitors (Lin et al., 2010) that provide unprecedented mobility for patients and provide doctors with real-time data that increases AF diagnosis accuracy and allows instant response to alarming events.

In a typical set-up, a wearable ECG monitor can be programmed to capture and wirelessly transmit raw ECG signals. However, transmitting raw data over energy-consuming wireless links severely reduces the sensor's battery life time. Currently available Wireless Body Sensor Networks (WBSN) platforms depend on limited batteries and it is essential to reduce as much as possible the inconvenience associated with battery replacements and recharges.

A key strategy is to implement 'energy-ware' signal processing algorithms on the sensor node. This way, the sensor node will only be required to transmit a minimal number of features instead of a full stream of raw data. However, the main challenge is to implement on-sensor signal processing within the constrained resources of a sensor node.

This paper, studies the feasibility of on-sensor AF features extraction. Instead of streaming ECG signals, the sensor locally extracts AF relevant features. When an AF episode is detected by the sensor it sends a

minimum number of bytes to alert the server. The underlying hypothesis evaluated in this paper is that low complexity on-sensor ECG signal processing can decrease the energy consumption of wireless transmission and therefore extend the lifetime of the sensor.

2 RELATED WORK

The electrical patterns, captured by the ECG (Petty, 2016), are manifested as a sequence of waveforms representing the sequence of contraction and relaxation of the heart. A normal cardiac cycle has distinct waveforms called the P wave, QRS complex and T wave as shown in Figure 1. The QRS complex is the most dominant feature of the ECG cycle with a sharp peak in the middle, called the R wave. A significant ECG feature is the interval between two consecutive R peaks, referred to as the RR interval.
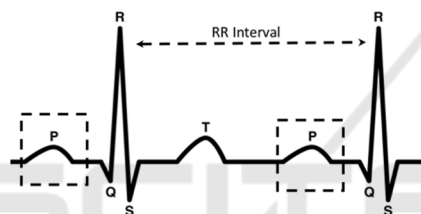

Figure 1: ECG Waveforms.

An ECG of a healthy heart shows a Normal Sinus Rhythm (NSR) where RR intervals are regular and the P waves are present. On the other hand, Atrial Fibrillation (AF) (January et al., 2014) is an irregular heart rhythm that is characterized on ECG signals by irregular RR intervals and absent P waves that are replaced by low-amplitude fibrillatory f-waves.

AF detection algorithms involve (Sörnmo, Petrenas, & Marozas, 2018): ECG pre-processing, AF features extraction, and finally classification. AF features are expected to quantify RR interval irregularity and/or provide information on the absence/presence of P and f waves. However, extracting reliable features that detect the presence/absence of P waves is challenging at low signal-to-noise ratios. Therefore, the majority of AF detection algorithms are RR-based and are designed to extract features that reflect the degree of randomness, variability, and complexity of RR interval series.

Commonly RR-based methods include comparing the density histogram of RR series to a standard density histogram (Tateno & Glass, 2002) and evaluating statistical attributes that reflect the

randomness and complexity of RR series (Dash, Chon, Lu, & Raeder, 2009). On the other hand, few contributions proposed P-wave based AF detectors. Ladavich et al. (Ladavich & Ghoraani, 2015) developed a rate-independent AF classifier that utilizes statistical and morphological features from a model of normal sinus rhythm P-wave ; whereas Ródenas et al. (Ródenas, García, Alcaraz, & Rieta, 2015) used wavelet entropy to quantify the presence/absence of P waves. AF detectors have also been designed to combine RR and P-wave features.

The AF detector proposed by Petrenas et. al (Petrėnas, Sörnmo, Lukoševičius, & Marozas, 2015) is based on four parameters that characterize RR interval irregularity, P wave absence, f wave presence, and the noise level in the signal. The algorithm presented in (de Carvalho et al., 2012) quantifies P wave absence by measuring the correlation of the detected P waves to a P wave model, assesses heart rate variability using a statistical similarity measure, and analyzes atrial activity using a wavelet approach. AF detection proposed by Babaeizadeh et. al (Babaeizadeh, Gregg, Helfenbein, Lindauer, & Zhou, 2009) involves a statistical classifier that uses as input a combination of P-R interval variability, a P wave morphology similarity measure, and an R-R Markov score. Regardless of the accuracy in AF detection, the previously mentioned contributions may not be technically feasible for real-time on-sensor processing of ECG signals due to the high computation requirements that can overwhelm the constrained sensor resources.

Therefore, we turned our attention to AF detection algorithms that have been designed to operate on wearable ECG monitors. The study in (Marsili et al., 2016) implements and tests an AF detection framework on a wearable prototype device. The study results demonstrate the framework capability to provide onboard AF detection with affordable computational burden. However, the detection approach is based solely on the RR feature and the prototype device used in the study is more resourceful than a constrained wearable sensor.

Rincon et al. (Rincon, Grassi, Khaled, Atienza, & Sciuto, 2012) implement AF detection on a WBSN platform by using fuzzy logic to combine the output of RR interval analysis and P-wave detection. The proposed approach demonstrated satisfactory accuracy but in terms of reducing energy consumption and extending the node lifetime, it offered a marginal 4% increase in the node's life time that does not play in favour of adopting it as an efficient energy solution.

3 EMBEDDED AF DETECTION

This section presents the specification of the proposed on-sensor AF detection algorithm. It describes the QRS detection algorithm in addition to the features extraction methods used to detect RR irregularity and absence of the P wave.

3.1 General Approach

In the proposed approach, the sensor processes a periodically acquired ECG segment to detect AF episodes. If an AF episode is detected, the sensor sends a notification to the server including relevant features (Figure 2). Recent medical studies (Rabinstein et al., 2013) highlighted the significance of detecting AF episodes that are shorter than 30 seconds. Therefore, the proposed scheme is based on the processing of a 10-seconds ECG signal. This length is an adequate recording length of the ECG signal that can contain a number of QRS complexes sufficient for extracting relevant AF features. From another side, the reduced set of samples in the processed ECG signal saves the memory in the wireless sensor. In addition, our approach is aligned with typical clinical settings, where a cardiologist examines a 10 seconds ECG strip (Meek & Morris, 2002).
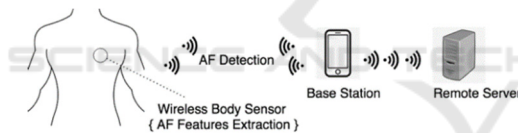

Figure 2: Proposed approach for embedded AF detection.

In the proposed approach, the QRS detection module detects the location of R peaks that act as reference point for further features extraction. On-sensor features extraction involves estimating the irregularity of RR intervals and detecting the presence/absence of the P wave. The embedded AF decision rules are applied to determine if the 10-seconds ECG signal is a possible AF episode. Once an AF episode is detected the sensor will send, to the base station, an alert notification in addition to the extracted relevant AF features. The base station will, in turn, forward the alert and AF features to a remote server for advanced ECG classification.

The vast majority of AF detection algorithms proposed in the literature are designed to classify individual heartbeats. However, the proposed scheme classifies a 10-seconds ECG segment that is composed of a number of heartbeats. This design choice is driven by the fact that an AF heartbeat does not occur in isolation but only as part of an AF episode.

3.2 QRS Detection

On-sensor ECG features extraction starts by detecting the QRS complex. For that purpose, we have adopted the Dual Slope algorithm (Wang, Deepu, & Lian, 2011) that analyses the signal in the time-domain and detects the signal segment that represents the QRS Complex. Once detected, we can extract R peaks from the QRS complex segment. The RR interval, as a relevant temporal feature, is extracted by measuring the time between two consecutive R peaks. In addition, we can use the R peak location to define a search window for the detection of the P wave presence/absence.

The Dual Slope algorithm does not require any QRS enhancement and directly starts detecting the QRS complex to localize the R peak. It focuses on calculating the slope of straight lines connecting two samples that are separated by a distance equal to the QRS width. The rationale behind slope calculation is that the largest value of slopes is expected to be found in the QRS complex.

3.3 AF Detection

AF episodes are reflected in ECG signals by irregularity of RR intervals and absence of valid P waves. The irregularity of RR intervals is measured using a simple statistic that gives an estimate of the standard deviation of RR intervals (eStd). When the eStd feature of the processed ECG segment crosses a pre-set threshold, the segment is labeled as having irregular RR intervals. Otherwise, the segment is labeled as having regular RR intervals.

A valid P wave would typically occur in the second half of the RR interval which we refer to as the search interval. The number of search intervals in a 10-seconds segment varies according to the heart rate. Therefore, we consider that there are N search intervals where N is equivalent to the number of RR intervals in the segment. From every search interval, the P wave detection algorithm extracts features that indicate if a valid P wave is absent or present. The algorithm maintains the number of search intervals that did not include a valid P wave (referred to as a Miss).

The number of Misses (M) is evaluated as a percentage of the total number of search intervals in the 10-seconds segment (N). The percentage can range from 0 to 100%. In our approach, the 10-seconds segment is assigned one of three

classification labels according to the percentage of Misses in that segment. Each classification label is associated with an interval on the real number line as depicted in Figure 3.

Figure 3: P-wave Miss Ratios and corresponding classification label.

To define the intervals, we need two values which we refer to as $\{ß_{Absent}, ß_{Present}\}$. If the percentage of Misses in the segment is in the interval $[ß_{Absent}, 100]$ then the segment is labeled "Absent" to reflect that the number of search intervals that did not have a valid P wave is high. The interval $[0, ß_{Absent}]$ covers two classification labels "Mostly Absent" and "Present". The label "Present" is assigned to segments in which the number of search intervals that did not have a valid P wave is low. The label "Mostly Absent" is assigned to segments in which the number of search intervals that did not have a valid P wave is in between the two extremes defined by the labels "Present" and the label "Absent". Therefore, to discriminate between the labels "Present" and "Mostly Absent" we define $ß_{Present}$ as the middle point of the interval $[0, ß_{Absent}]$ given by $(\frac{ß_{Absent}}{2})$. The values $\{ß_{Absent}, ß_{Present}\}$ are experimentally evaluated as later show in section 4. Figure 4 illustrates the labeling of the segment according to the values $\{ ß_{Absent}, ß_{Present}\}$.
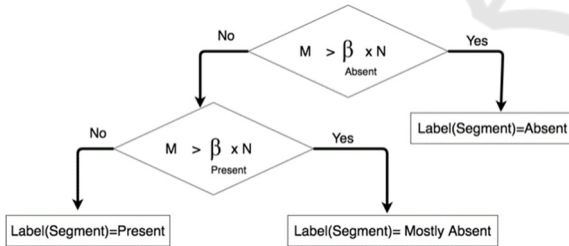

Figure 4: Classification labels based on P wave Detection.

3.3.1 RR Analysis

The RR feature is evaluated as the time interval between two consecutive R peaks. To capture RR irregularity, we used a simple statistical measurement (Bluman, 2009) that gives an estimate of the standard deviation (Std) of RR intervals (1). We refer to this measurement as eStd (RRs) where RRs is the set of RR intervals extracted from the 10-seconds ECG signal.

$$eStd\,(RRs) = \frac{\max\,(\,RR_s\,) - \min\,(\,RR_s\,)}{4} \qquad (1)$$

The process of irregularity detection is based on the comparison of eStd (RRs) value of a 10-seconds ECG signal with a pre-set threshold (TH_{Std}). To estimate the value of the threshold (TH_{Std}) we used 268 10-seconds segments of ECG signals that were annotated with AF episodes in the MIT/BIH Arrhythmia Database (G. Moody & Mark, 2001). Figure 5 shows the distribution of eStd values in ECG segments that are entirely AF episodes. No Normal Sinus Rhythm (NSR) segments were included in the analysis. According to the figure the majority of AF eStd values measured (82%) were greater than 0.04. Therefore, TH_{Std} is set to the value of 0.04.
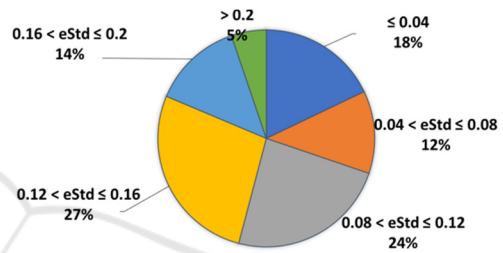

Figure 5: Distribution of eStd values in AF episodes.

To validate the eStd measurement capability in capturing RR irregularity, we used a set of variable length ECG segments: 10 seconds, 20 seconds, and 30 seconds. Experiments have shown that as the segments get longer than 10 seconds, the correlation between eStd and classical Std starts to decrease. Thus, we can conclude that RR irregularity can be detected in an ECG segment as short as 10 seconds. This signal length implies lower memory requirements, less processing time and eventually lower energy consumption.

3.3.2 P wave Detection

In the proposed AF detection scheme, we are not interested in detecting the temporal location of P wave fiducial points. Instead, we are investigating: "Is there a valid P wave in the current search interval?". To answer this question, a wavelet transformation is performed to approximate the morphology of the second half of the RR interval (search interval). The idea is that if the approximation extracted is similar to a pre-defined template of a valid P wave then we can say that a P wave is present in the search interval. Otherwise, the P wave is considered absent.

The Haar wavelet (Walker, 2008) is the simplest type of wavelet that decomposes a discrete signal into two sub-bands where each sub-band is half the length of the original signal. The first sub band is a running average that approximates the shape of the original signal. The second sub band contains the difference that generates the detail coefficients.

Rincon et. al (Rincon et al., 2012) adopted the quadratic spline wavelet (Martínez, Almeida, Olmos, Rocha, & Laguna, 2004) to delineate the ECG signal. For that purpose the sensor is expected to maintain 5 levels of wavelet decomposition including both approximation and detail coefficients. To keep the time-invariance and temporal resolution at different scales, the same sampling rate has been used in all scales.

In the proposed scheme we have selected the Haar wavelet for its computational effeciency (Mazomenos et al., 2013). Moreover, the sensor is designed to maintain only the approximation coefficients at level 2. Experiments have shown that 2 levels provide adequate noise reduction. The pseudocode of P wave Haar based approximation is illustrated in Figure 6.

In contrast to the wavelet approach adopted by Rincon et. al (Rincon et al., 2012), Haar based approach is lighter in terms of memory requirements and computational complexity. This is due to the simplicity of the Haar wavelet in addition to the fact that the wavelet decomposition is only applied to a small portion of the signal. This setup translates to lower energy consumption.

```
P: P wave , P̂ : approximated P wave
N = length(P)
i = 1
j = 1
while(i < N)
   P̂ (j) = (P(i) + P(i + 1) ) / √2
   i = i + 2
   j = j + 1
end
```

Figure 6: A single level Haar approximation.

To create a template of the P wave, we have used the set of NSR signals (Table 1) in the QT database (Laguna, Mark, Goldberger, & Moody, 1997). From each signal, we have used 1 minute of ECG recording with an average number of 50 P waves per signal. P waves were extracted as the second half of the RR intervals marked by the Dual Slope algorithm. Then a 2-level Haar transform was applied to each P wave to obtain an approximation of the P wave. The template P wave was chosen as the average of the 400+ approximated P waves extracted from the signals.

Table 1: NSR signals used in P wave template.

sel16265	sel16272	sel16273
sel16420	sel16773	sel16539
sel16786	sel17152	sel17453

To ensure the scalability of the template, we have normalized the sample amplitudes. This is a necessary step since the amplitude values will vary among signals according to the technology used in recording the ECG signal. We have used min-max scaling to rescale amplitudes to the unified scale [-1,1].

The extracted P waves and the template P wave are different in length. In addition, the length of extracted P waves varies according to the heart rate that defines the duration of an RR interval. Therefore, we have selected Dynamic Time Warping (DTW) (Li, 2014) which is able to measure the distance between time series of unequal length and that are not aligned in time. With Dynamic Time Warping we are able to compare any P wave to the template P wave regardless of the heart rate and the sampling frequency of the input signal. If the distance is within a pre-set threshold (TH_{DTW}), then approximated P wave ($\hat{P}$) is accepted as a valid P wave. Otherwise, the P wave is considered absent.

To evaluate threshold (TH_{DTW}), we used two sets of signals (Table 2): AF signals obtained from the MIT Atrial Fibrillation Database (G. B. Moody & Mark, 1983)(Goldberger et al., 2000) and non-AF signals obtained from MIT-BIH Normal Sinus Rhythm database (Goldberger et al., 2000). AF signals were extracted as entirely AF episodes that ranged in duration from 25 seconds to 100 seconds. The total duration of AF episodes was around 8 minutes. NSR signals were in total 10 minutes long with 200 seconds per database record. In total there were 690 AF distances and 830 NSR distances.

Table 2: Signals used for TH_{DTW} evaluation.

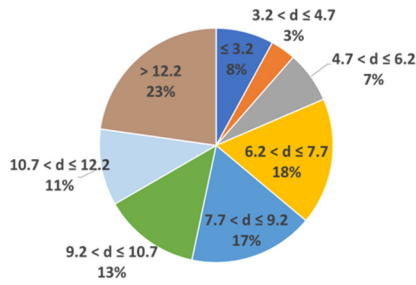| AF Signals	04048, 05121, 08215, 04043, 04746, 06453
NSR Signals	19830, 16483, 16795

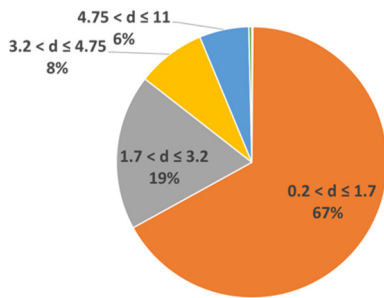Figure 7: Distribution of DTW distances in AF signals.

Figure 8: Distribution of DTW distances in NSR signals.

Figure 7. reflects the frequency of distances obtained from AF signals. Only (8%) of the distances were less than or equal to 3.2. The majority of the distances (92%) were greater than 3.2.

On the other hand, Figure 8 plots the distribution of distances obtained from NSR signals. Only (14%) of the distances were greater than 3.2. The majority of the distances (86%) were less than equal to 3.2. Therefore, we can conclude that the value 3.2 is reasonable threshold since the majority of AF distances were greater than 3.2 while the majority of NSR distances were less than or equal to 3.2.

3.3.3 AF Decision Rules

The features extraction module of the proposed scheme will produce two classification labels for each 10-seconds segment. These output labels will be used to classify the segment as AF or non-AF (Table 3).

Table 3: AF rule- based classifier using RR and P wave features.

AF Classifier		P wave Labels		
		Present	Mostly Absent	Absent
RR Labels	Regular	non-AF *(Rule1)*	non-AF *(Rule3)*	noisy *(Rule4)*
	Irregular	non-AF *(Rule5)*	AF *(Rule6)*	AF *(Rule2)*

Rule (1) will capture definite cases of Normal Sinus rhythm that is characterized by regular RR intervals and a valid P waves preceding each QRS complex. Rule (2) will capture definite cases of Atrial Fibrillation rhythm that is characterized by irregular RR intervals and QRS complexes that are not preceded by valid P waves.

In Rules (3) and (4), more weight is given to the RR feature. Therefore, the segment is classified as non-AF in Rule (3) and the absence of P waves is attributed to noise. Rule (4) classifies the segment as noisy since the P waves are said to be entirely absent.

Rules (5) and (6) apply for segments in which RR intervals are irregular. In Rule (5), more weight is given to the P wave feature. Therefore, the segment is classified as non-AF. However, Rule (6) classifies the segment as AF since most of the time the P wave is absent.

4 PERFORMANCE ANALYSIS

The objective of our algorithm to efficiently discriminate between Normal Sinus Rhythm (NSR) and Atrial Fibrillation (AF) rhythm. Therefore, the test signals (Table 4) do not include any other arrhythmia such as Atrial Flutter. In addition, each segment is either entirely NSR or AF. There is no overlapping between segments.

Table 4: Test signals (AF Detection).

AF	04015, 07910, 04126, 04908
NSR	18177, 18184, 19088, 19090, 19093, 19140

We calculated two performance metrics of detection accuracy: Sensitivity (Se) and Specifity (Sp). Sensitivity defines the percentage of AF segments that were correctly classified (2) whereas the specificity defines the percentage of non-AF segments that were correctly classified (3).

$$Se = \frac{TP}{TP+FN} \qquad (2)$$

$$Sp = \frac{TN}{TN+FP} \qquad (3)$$

As previously explained in section 3.2, the detection of the P wave is based on the design parameter β that represents the percentage of Misses in a 10-seconds segment. For the purpose of this evaluation, we run the P wave based AF detection algorithm at different values of β. Table 5

summarizes the AF detection results at β = 0.3, 0.4, 0.5, 0.6, and 0.7 respectively.

Table 5: AF Detection accuracy based only on P wave.

	β				
	0.3	0.4	0.5	0.6	0.7
Se %	99.8	99.2	98.5	96.4	92.9
Sp%	71.6	80.9	88.5	93.9	97.2

We can conclude from Table 5 that the best performance was at β = 0.6 and β = 0.7 where both Sensitivity and Specifity values are above 90% However, the performance metrics at β = 0.6 are considered better since they give a higher Se 96 %, even though it is less specific (93 %). A lower Se might allow some AF cases to pass with no alarm. However, lower Sp means that non-AF cases might create some false-alarms. A false harm-less alarm is more desirable than a harmful no-alarm.

The combination of features is performed according to the classification rules summarized in Table 3. The highest pair of Se and Sp achieved by the wavelet based P wave detector was at β = 0.6 (Se = 96.4% and Sp = 93.89%). Therefore, we can set β_{Absent} to 0.6 and $\beta_{Present} = (\frac{\beta_{Absent}}{2}) = 0.3$.

In comparison to related work in the area of embedded AF detection, we can observe from Table 6 that the proposed approach for on-sensor AF detection using the combination of eStd and P-wave features is comparable to related work.

Table 6: Comparison of proposed approach to related work in embedded AF detection.

AF Detection Approaches	Se %	Sp %
using eStd only	80.68	94.81
using P-wave only	96.4	93.89
using eStd and P-wave	98.59	97.61
AF detection on Teleholter device (Marsili et al., 2016)	97.33	98.67
AF detection on Shimmer platform (Rincon et al., 2012)	96	93

5 ENERGY EVALUATION

The underlying hypothesis evaluated in this paper is that an efficient on-sensor processing of the ECG signal increases the battery life time and ensures the longevity of the application. Therefore it is important to evaluate the energy consumption of (a) the classical approach of full ECG transmission in contrast to (b) the proposed approach of on-sensor AF detection. The sensing energy is constant in both scenarios. Therefore, we focus on evaluating the energy consumed by local processing and wireless transmission. For the purpose of evaluation, we assume a 12-bit ADC with sampling frequency (S_F=250 Hz).

Table 7: Energy consumption of AF detection scheme.

Module	Energy Label	Energy units (mJ)	per unit
R peak detection	E_{sample}	0.03	energy per sample
	E_R	75	energy per segment
RR interval extraction	E_{RR}	0.01	energy per RR
P wave detection	E_P	1.2	energy per RR
AF features Extraction	E_{FX}	19	energy per segment
AF detection	E_{AF}	0.87	energy per segment
Server Notificaiton	E_{radio}	0.3	energy per byte
	$E_{radioSample}$ (2 bytes)	0.6	energy per sample
	$E_{radioRR}$ (4 bytes)	1.2	energy per RR

Table 7. lists the estimated energy cost of each module in the proposed AF detection scheme using the Avrora tool (Avrora, 2008) that provides a cycle-accurate simulation of the AVR microcontroller. Note that this evaluation considers the worst algorithmic case of each module.

Local ECG processing is composed of R peak detection (E_R), AF features extraction (E_{FX}), and AF decision (E_{AF}). E_R is the amount of energy consumed to detect R peaks in a 10-seconds segment = 75 mJ. E_{AF} is the amount of energy consumed by the rule-based classifier = 0.87 mJ. E_{FX} is the amount of energy consumed to extract RR and P wave features equal to 19 mJ.

The total energy consumed for processing of a 10 seconds ECG segment given by (4):

$$E_{AF10s} = E_R + E_{FX} + E_{AF} = 94.87 \ mJ \qquad (4)$$

In the classical approach of full ECG transmission, the energy is consumed by radio transmission as there is no local ECG processing. Therefore, the total energy consumed in this scenario ($E_{ECG\_transmission(a)}$) is around 45 J.

On the other hand, if we consider that the sensor performs periodic on-node AF detection every 10 seconds for 5 minutes ECG signal then the total energy for the processing of the proposed AF detection scheme $E_{AFTotal(b)}$ = 3.4 J

The gain in energy saving measured by :

$$G = \left(1 - \frac{E_{AFTotal(b)}}{E_{ECG\_transmission}_{(a)}} \right) *100 = 92.5 \ \% \qquad (5)$$

This gain in energy saving (5) shows that our proposed scheme for embedded Atrial Fibrillation detection achieves a considerable gain in the energy consumed for AF detection when compared to the classical approach based on the full transmission of the ECG signal to a remote server for analysis. In fact, the energy gain achieved is higher than the marginal 4% increase in the battery life time reported by Rincon et. al (Rincon et al., 2012).

We note that the gain in energy consumption increases as the ratio $\frac{T_{ECG}}{T_{AF}}$ decreases. Which means as we increase the periodicity of AF detection we increase the gain in energy. However, we have to keep in mind the trade-off between AF detection efficiency and energy saving to extend the network life time. In practice, this periodicity should be based on clinical requirements.

6 CONCLUSIONS

This paper presents a new approach of on-sensor AF detection as a data reduction strategy. In this approach, the body sensor node is designed to efficiently extract and analyze relevant ECG features in order to classify the ECG signal as a possible AF episode. This decision will be submitted to the remote server with the minimum representation of data to perform further classification. Performance results have shown that the proposed scheme achieved high sensitivity (98.59%) and specificity (97.61%) demonstrating high accuracy in the detection of the AF episodes. In comparison with the transmission of full ECG signals, the proposed approach can save around 92% of energy. For future work, we are considering hardware implementation of the proposed system in FPGA platform.

ACKNOWLEDGEMENTS

REFERENCES

Avrora. (2008). Avrora - The AVR Simulation and Analysis Framework. Retrieved July 20, 2016, from http://compilers.cs.ucla.edu/avrora/

Babaeizadeh, S., Gregg, R. E., Helfenbein, E. D., Lindauer, J. M., & Zhou, S. H. (2009). Improvements in atrial fibrillation detection for real-time monitoring. *Journal of Electrocardiology*, *42*(6), 522–526. https://doi.org/10.1016/j.jelectrocard.2009.06.006

Bluman, A. G. (2009). *Elementry Statistics: A Step by Step Approach* (7th ed.). McGraw-Hill.

Dash, S., Chon, K., Lu, S., & Raeder, E. (2009). Automatic Real Time Detection of Atrial Fibrillation. *Annals of Biomedical Engineering*. https://doi.org/10.1007/s10439-009-9740-z

de Carvalho, P., Henriques, J., Couceiro, R., Harris, M., Antunes, M., & Habetha, J. (2012). *Model-Based Atrial Fibrillation Detection. ECG Signal Processing, Classification and Interpretation: A Comprehensive Framework of Computational Intelligence.* https://doi.org/10.1007/978-0-85729-868-3

Goldberger, A. L., Amaral, L. A. N., Glass, L., Hausdorff, J. M., Ivanov, P. C., Mark, R. G., … Stanley, H. E. (2000). PhysioBank, PhysioToolkit, and PhysioNet: Components of a New Research Resource for Complex Physiologic Signals. *Circulation 101(23)*, e215–e220.

Retrieved from http://circ.ahajournals.org/content/101/23/e215.full

January, C. T., Wann, L. S., Alpert, J. S., Field, M. E., Calkins, H., Murray, K. T., … Sellke, F. W. (2014). *2014 AHA / ACC / HRS Guideline for the Management of Patients With Atrial Fibrillation*. https://doi.org/10.1161/CIR.0000000000000041

Ladavich, S., & Ghoraani, B. (2015). Rate-independent detection of atrial fibrillation by statistical modeling of atrial activity. *Biomedical Signal Processing and Control*, *18*, 274–281. https://doi.org/10.1016/j.bspc.2015.01.007

Laguna, P., Mark, R. G., Goldberger, A., & Moody, G. B. (1997). A Database for Evaluation of Algorithms for Measurement of QT and Other Waveform Intervals in the ECG. *Computers in Cardiology*, *24*, 673–676.

Li, H. (2014). On-line and dynamic time warping for time series data mining. *International Journal of Machine Learning and Cybernetics*, *6*(1), 145–153. https://doi.org/10.1007/s13042-014-0254-0

Lin, C. T., Chang, K. C., Lin, C. L., Chiang, C. C., Lu, S. W., Chang, S. S., … Ko, L. W. (2010). An intelligent telecardiology system using a wearable and wireless ecg to detect atrial fibrillation. *IEEE Transactions on Information Technology in Biomedicine*, *14*(3), 726–733. https://doi.org/10.1109/TITB.2010.2047401

Mairesse, G. H., Ireland, P. M., Gelder, I. C. Van, Germany, C. E., Uk, J. M., & Uk, A. B. (2018). Screening for atrial fibrillation : a European Heart Rhythm Association (EHRA) consensus document, (March), 1589–1623. https://doi.org/10.1093/europace/eux177

Marsili, I. A., Masè, M., Pisetta, V., Ricciardi, E., Andrighetti, A. O., Ravelli, F., & Nollo, G. (2016). Optimized Algorithms for Atrial Fibrillation Detection by Wearable Tele-Holter Devices. In *2016 IEEE International Smart Cities Conference (ISC2)*.

Martínez, J. P., Almeida, R., Olmos, S., Rocha, A. P., & Laguna, P. (2004). A Wavelet-Based ECG Delineator : Evaluation on Standard Databases. *IEEE Transactions on Biomedical Engineering*, *51*(4), 570–581.

Mazomenos, E. B., Biswas, D., Acharyya, A., Chen, T., Maharatna, K., Rosengarten, J., … Curzen, N. (2013). A Low-Complexity ECG Feature Extraction Algorithm for Mobile Healthcare Applications. *IEEE Journal of Biomedical and Health Informatics*, *17*(2), 459–469.

Meek, S., & Morris, F. (2002). ABC of clinical electrocardiography.Introduction. I-Leads, rate, rhythm, and cardiac axis. *BMJ (Clinical Research Ed.)*, *324*(7334), 415–418. https://doi.org/10.1136/bmj.324.7334.415

Moody, G. B., & Mark, R. G. (1983). A new method for detecting Atrial Fibrillation using RR intervals. *Computers in Cardiology*, *10*, 227–230.

Moody, G., & Mark, R. (2001). The impact of the MIT-BIH Arrhythmia Database. *IEEE Engineering in Medicine and Biology Magazine*, *20*(3), 45–50.

Petrėnas, A., Sörnmo, L., Lukoševičius, A., & Marozas, V. (2015). Detection of occult paroxysmal atrial fibrillation. *Medical and Biological Engineering and Computing*, *53*(4), 287–297. https://doi.org/10.1007/s11517-014-1234-y

Petty, B. G. (2016). *Basic Electrocardiography*. New York: Springer.

Rabinstein, A. A., Fugate, J. E., Mandrekar, J., Burns, J. D., Seet, R. C. S., Dupont, S. A., … Friedman, P. A. (2013). Paroxysmal Atrial Fibrillation in Cryptogenic Stroke-A Case Control Study. *Journal of Stroke & Cerebrovascular Diseases*, *22*(8), 1405–1411.

Rincon, F., Grassi, P. R., Khaled, N., Atienza, D., & Sciuto, D. (2012). Automated Real-Time Atrial Fibrillation Detection on a Wearable Wireless Sensor Platform. In *34th Annual International Conference of the IEEE EMBS* (pp. 2472–2475).

Ródenas, J., García, M., Alcaraz, R., & Rieta, J. J. (2015). Wavelet Entropy Automatically Detects Episodes of Atrial Fibrillation from Single-Lead Electrocardiograms. *Entropy*, *17*, 6179–6199. https://doi.org/10.3390/e17096179

Sörnmo, L., Petrenas, A., & Marozas, V. (2018). Atrial Fibrillation from an Engineering Perspective. In L. Sörnmo (Ed.) (1st ed., p. 316). Springer International Publishing.

Tateno, K., & Glass, L. (2002). A method for detection of atrial fibrillation using RR intervals. https://doi.org/10.1109/cic.2000.898539

Walker, J. S. (2008). *A Primer on Wavelets and Their Scientific Applications* (2nd ed.). CRC Press.

Wang, Y., Deepu, C. J., & Lian, Y. (2011). A Computationally Efficient QRS Detection Algorithm for Wearable ECG Sensors. In *Engineering in Medicine and Biology Society, EMBC, 2011 Annual International Conference of the IEEE* (pp. 5641–5644).